JOURNAL OF COMPUTATIONAL PHYSICS 2, 198-222 (1967)

Finite-Difference Calculations for Hydrodynamic Flows Containing Discontinuities[1,2]

SAMUEL Z. BURSTEIN

Courant Institute of Mathematical Sciences,
New York University

ABSTRACT

In this paper it is shown how to calculate the steady hypersonic inviscid flow, including a detached shock, around a blunt body. The steady flow is obtained as the limit for large time of time-dependent flow, starting with plane flow impinging on the body. The transient flow is the solution of a mixed initial–boundary-value problem for the partial differential equations of inviscid fluids which is solved by a difference scheme proposed by Lax and Wendroff. Our calculations show that by itself this difference scheme tends to be unstable and does not converge to the steady flow; by adding an artificial viscosity term we have succeeded in stabilizing the calculation. Section 4 is a fairly convincing theoretical explanation of this stabilizing effect and a new stability condition is derived.

Both plane and cylindrical symmetries are considered; in the cylindrical case a variant of Richtmyer's [4] two-step version of the Lax-Wendroff difference scheme is used. This method, as does Richtmyer's, requires much fewer arithmetic operations as compared with the one-step method.

[1] Contract No. AT(30–1)–1480.

[2] This report was prepared as an account of Government-sponsored work. Neither the United States, nor the Commission, nor any person acting on behalf of the Commission: (A) makes any warranty or representation, express or implied, with respect to the accuracy, completeness, or usefulness of the information contained in this report, or that the use of any information, apparatus, method, or process disclosed in this report may not infringe privately owned rights; or (B) assumes any liabilities with respect to te use of any information, apparatus, method, or process disclosed in this report.

As used in the above, "person acting on behalf of the Commission" includes any employee or contractor of the Commission, or employee of such contractor, to the extent that such employee or contractor of the Commission, or employee of such contractor prepares, disseminates, or provides access to, any information pursuant to his employment or contract with the Commission, or his employment with such contractor.

1. Introduction

This report continues the exploration of certain explicit difference methods for fluid dynamic computations in three independent variables. The application of the Lax–Wendroff method was extended to a more difficult problem the detached shock problem. The method of solution is to consider the problem to be of the mixed type, an initial- and boundary-value problem. By prescribing boundary-conditions both on the body and at the upstream and downstream regions and by prescribing the initial data, a time-dependent solution was generated from the above conditions. Solutions for large times were obtained and these correspond to the steady state. Both plane and axisymmetric flows were considered, and several difference methods were tested and compared.

In a previous paper [1] results were presented for a series of calculations relating to compressible flows in channels. These flows contain oblique shocks and, for some shapes, Mach reflections. It was noted that if Mach reflection took place, there were oscillations present in the downstream region of the flow field, i.e., behind the normal shock wave and extending to the boundary; no such oscillations were detected for the case of regular reflection. It might be thought that the difference between the two cases can be tentatively explained as follows: the treatment of the downstream boundary by extrapolation-introduced errors. In subsonic flow these errors propagate upstream and affect the accuracy of the solution but are swept out of the mesh in supersonic flows.

However, severe difficulties were encountered in the numerical calculation of the detached shock problem. The solution of these difficulties shed light on the behavior of the difference equations and, in return, on the nature of the oscillations encountered in the Mach reflection calculation.

2. Hydrodynamic Differential Equations

The conservation of mass, momentum, and energy in inviscid time-dependent fluid motion is expressed by equations of divergence form

$$\operatorname{div} \boldsymbol{\varphi} = 0 . \tag{2.1}$$

Here

$$\boldsymbol{\varphi} = (\mathbf{w}, \mathbf{f}(\mathbf{w}), \mathbf{g}(\mathbf{w})) \tag{2.2}$$

and div is the partial operator in three-dimensional space–time

$$\operatorname{div} = (\quad)_{,t} + (\quad)_{,x} + (\quad)_{,y} . \tag{2.3}$$

Hence

$$\mathbf{w}_{,t} + \mathbf{f}_{,x} + \mathbf{g}_{,y} = 0\,,$$

and **w**, **f**, and **g** are vectors. The components of **w** are mass, momentum in the x- and y-direction, and the total energy, all per unit volume, i.e.,

$$\mathbf{w} = \begin{pmatrix} \varrho \\ \varrho u \\ \varrho v \\ E \end{pmatrix}.$$

The vectors **f** and **g** are nonlinear vector-valued functions corresponding to the fluxes in the x- and y-directions of the quantities **w**.

For the case of axially symmetric flows the equations of motion take the slightly different form,

$$\operatorname{div} \boldsymbol{\varphi} = \mathbf{h}, \tag{2.4}$$

where the vector $\mathbf{h} = -v/y\,(\mathbf{w} + \boldsymbol{\pi})$, $\boldsymbol{\pi}^T = (0, 0, 0, p)$ and the coordinate y stands for the radial distance from the axis of symmetry. Equation (2.4) may be written in almost conservation form if the vector $\mathbf{s}^T = (0, 0, p, 0)$ is introduced by

$$-y\mathbf{h} + \begin{pmatrix} 0 \\ 0 \\ p \\ 0 \end{pmatrix} \equiv \mathbf{g}\,. \tag{2.5}$$

Expanding Eq. (2.4) by using the relations (2.2), (2.3), (2.4), and (2.5) yields

$$\mathbf{w}_{,t} + \mathbf{f}_{,x} + \mathbf{g}_{,y} = -\mathbf{s}\,. \tag{2.6}$$

Thus the vector $\boldsymbol{\varphi}$ is replaced by $y\boldsymbol{\varphi}$ in Eq. (2.4), while the inhomogeneous term **s** contains only one nonzero component in the radial momentum equation compared to four contained in **h**. For net points not on the axis of symmetry, Eq. (2.6) should be used for the generation of the difference scheme in axially symmetric flows.

The pressure p may be expressed in terms of the conservation variables and the ratio of specific heats of the gas ,γ, through

$$p = (\gamma - 1)\,\{E - (m^2 + n^2)/2\varrho\}, \tag{2.7}$$

where $m = \varrho u$ and $n = \varrho v$. With the use of Eq. (2.7), the vectors $\mathbf{f}(\mathbf{w})$ and $\mathbf{g}(\mathbf{w})$ become

$$\mathbf{f}(\mathbf{w}) = \begin{bmatrix} m \\ -\frac{\gamma-3}{2}\frac{m^2}{\varrho} + (\gamma-1)\left\{E - \frac{1}{2}\frac{n^2}{\varrho}\right\} \\ \frac{mn}{\varrho} \\ \frac{(1-\gamma)}{2} m(m^2+n^2) + \gamma\frac{mE}{\varrho} \end{bmatrix},$$

$$\mathbf{g}(\mathbf{w}) = \begin{bmatrix} n \\ \frac{nm}{\varrho} \\ -\frac{\gamma-3}{2}\frac{n^2}{\varrho} + (\gamma-1)\left\{E - \frac{1}{2}\frac{m^2}{\varrho}\right\} \\ \frac{1-\gamma}{2} n(n^2+m^2) + \gamma\frac{nE}{\varrho} \end{bmatrix}.$$

For axially symmetric flows, ϱ is replaced by $y\varrho$ everywhere in the above expressions.

3. Difference Schemes of Second-Order Accuracy

The difference scheme that Lax and Wendroff used for one-dimensional calculations [3] and for the two-dimensional version which was analyzed in [2] is based on the Taylor expansion

$$\mathbf{w}(t + \Delta t) = \mathbf{w}(t) + \Delta t\, \mathbf{w}_{,t} + \Delta t^2/2\, \mathbf{w}_{,tt}\,. \tag{3.1}$$

The error in the above expression is third-order in the time interval Δt. The second term may be evaluated by substitution of the differential equation (2.3). If (2.3) is differentiated with respect to the independent variable time, then $-\mathbf{w}_{,tt}$ is given by

$$\begin{aligned} (\mathbf{f}_{,x} + \mathbf{g}_{,y})_{,t} &= (\mathbf{f}_{,t})_{,x} + (\mathbf{g}_{,t})_{,y} \\ &= \left(\frac{\partial \mathbf{f}}{\partial \mathbf{w}}\mathbf{w}_{,t}\right)_{,x} + \left(\frac{\partial \mathbf{g}}{\partial \mathbf{w}}\mathbf{w}_{,t}\right)_{,y} \\ &\equiv [\mathbf{A}(\mathbf{f}_{,x} + \mathbf{g}_{,y})]_{,x} + [\mathbf{B}(\mathbf{f}_{,x} + \mathbf{g}_{,y})]_{,y}\,. \end{aligned} \tag{3.2}$$

In (3.2) the matrices **A** and **B** are the Jacobians $\mathbf{f}_{,\mathbf{w}}$ and $\mathbf{g}_{,\mathbf{w}}$ respectively, and are given by

$$\mathbf{A}(\mathbf{w}) = -\begin{bmatrix} 0 & -1 & 0 & 0 \\ \frac{3-\gamma}{2}X^2+\frac{1-\gamma}{2}Y^2 & (\gamma-3)X & (\gamma-1)Y & (1-\gamma) \\ XY & -Y & -X & 0 \\ \gamma XZ+(1-\gamma)X(X^2+Y^2) & -\gamma Z+\frac{\gamma-1}{2}(3X^2+Y^2) & (\gamma-1)XY & -\gamma X \end{bmatrix}, \tag{3.3}$$

$$\mathbf{B}(\mathbf{w}) = -\begin{bmatrix} 0 & 0 & -1 & 0 \\ XY & -Y & -X & 0 \\ \frac{3-\gamma}{2}Y^2+\frac{1-\gamma}{2}X^2 & (\gamma-1)X & (\gamma-3)Y & (1-\gamma) \\ \gamma YZ+(1-\gamma)Y(X^2+Y^2) & (\gamma-1)XY & -\gamma Z+\frac{\gamma-1}{2}(3Y^2+X^2) & -\gamma Y \end{bmatrix}.$$

The abbreviations

$$X = m/\varrho, \quad Y = n/\varrho, \quad Z = E/\varrho$$

have been used.

Equations (2.3) and (3.2), when substituted into (3.1), yield

$$\begin{aligned} \mathbf{w}(t+\Delta t) = \mathbf{w}(t) &+ \Delta t(\mathbf{f}_{,x} + \mathbf{g}_{,y}) \\ &+ \frac{\Delta t^2}{2}\{[\mathbf{A}(\mathbf{f}_{,x} + \mathbf{g}_{,y})]_{,x} + [\mathbf{B}(\mathbf{f}_{,x} + \mathbf{g}_{,y})]_{,y}\}. \end{aligned} \tag{3.3'}$$

We are using (2.1) in the form $\mathbf{w}_{,t} = \mathbf{f}_{,x} + \mathbf{g}_{,y}$.

To preserve the high-order accuracy, the terms containing first derivatives must be approximated by centered differences and the term containing the second derivatives, since it is $o(\Delta t^2)$, may be approximated by uncentered differences. However, to center the entire expression, consider the vectors **C** evaluated at the half interval (see Fig. 1a):

$$\begin{aligned} \mathbf{C}(\Delta X/2) = \frac{\mathbf{f}(x^+, y) + \mathbf{f}(x, y)}{2} &+ \frac{\lambda}{4}(\mathbf{A}^+ + \mathbf{A})\{\mathbf{f}(x^+, y) - \mathbf{f}(x, y) \\ &+ \tfrac{1}{4}[\mathbf{g}(x^+, y^+) + \mathbf{g}(x, y^+) - \mathbf{g}(x^+, y^-) - \mathbf{g}(x, y^-)]\}. \end{aligned} \tag{3.4a}$$

To form $\mathbf{C}(-\Delta X/2)$, we wish to translate the argument X by the amount $-\Delta X$. Multiplication by the translation operator T gives

$$\mathbf{C}(-\Delta X/2) = T_{-1}^{(X)}\,\mathbf{C}(\Delta X/2). \tag{3.4b}$$

Similarly, in the y-direction

$$\mathbf{C}(\Delta Y/2) = \frac{\mathbf{g}(x, y^+) + \mathbf{g}(x, y)}{2} + \frac{\lambda}{4}(\mathbf{B}^+ + \mathbf{B})\,\{\tfrac{1}{4}[\mathbf{f}(x^+, y^+) + \mathbf{f}(x^+, y) - \mathbf{f}(x^-, y^+) - \mathbf{f}(x^-, y)] + \mathbf{g}(x, y^+) - \mathbf{g}(x, y)\}\,, \tag{3.4c}$$

and

$$\mathbf{C}(-\Delta Y/2) = T_{-1}^{(Y)}\,\mathbf{C}(\Delta Y/2). \tag{3.4d}$$

We have used the notation $\mathbf{A}^+ = \mathbf{A}(x + \Delta x)$, $\mathbf{B}^+ = \mathbf{B}(y + \Delta y)$, etc. Then the difference approximation to Eq. (2.1) is

$$\mathbf{w}(t + \Delta t) = \mathbf{w}(t) + \lambda\,\{[\mathbf{C}(\Delta X/2) - \mathbf{C}(-\Delta X/2)] + [\mathbf{C}(\Delta Y/2) - \mathbf{C}(-\Delta Y/2)]\}\,. \tag{3.5}$$

Here $\lambda = \Delta t/\Delta$ where $\Delta = \Delta x = \Delta y$. It is seen then, that by centering, the difference scheme has one of the properties of the differential equation; it is in divergence free form.

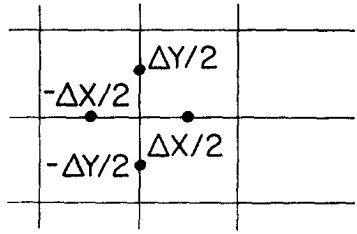

FIG. 1a

The solution of the axially symmetric equations can be achieved more simply by a two-step calculation analogous to the one developed by Richtmyer [4]. Two-step methods have the advantage of not requiring the computation of the matrices **A** and **B** and hence matrix-vector multiplication is eliminated. A variant of the two-step Lax–Wendroff scheme in two dimensions is:

Step 1: generates temporary data at the four points $(\cdot)$ $(k = i \pm \frac{1}{2}, l = j \pm \frac{1}{2}, t + \Delta t)$ from the nine points (x) shown in Fig. 1b from

$$\begin{aligned}\mathbf{w}_{k,l}(t + \Delta t) = \tfrac{1}{4}(&\mathbf{w}_{k+1/2,l+1/2} + \mathbf{w}_{k+1/2,l-1/2} + \mathbf{w}_{k-1/2,l+1/2} \\ &+ \mathbf{w}_{k-1/2,l-1/2}) + \frac{\lambda}{2}\{\mathbf{f}_{k+1/2,l+1/2} - \mathbf{f}_{k-1/2,l+1/2} \\ &+ \mathbf{f}_{k+1/2,l-1/2} - \mathbf{f}_{k-1/2,l-1/2}) + \frac{\lambda}{2}\{\mathbf{g}_{k+1/2,l+1/2} - \mathbf{g}_{k+1/2,l-1/2} \\ &+ \mathbf{g}_{k-1/2,l+1/2} - \mathbf{g}_{k-1/2,l-1/2}).\end{aligned} \tag{3.6}$$

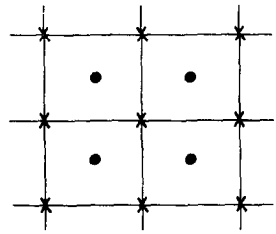

FIG. 1b

Step 2: gives the final result in terms of the data at the nine points shown in Fig. 1b′ from

$$\begin{aligned}\mathbf{w}_{i,j}(t + \Delta t) = \mathbf{w}_{i,j}(t) &+ \frac{\lambda}{4}(\mathbf{f}_{i+1,j} - \mathbf{f}_{i-1,j} + \mathbf{f}_x^{t+\Delta t}) \\ &+ \frac{\lambda}{4}(\mathbf{g}_{i,j+1} - \mathbf{g}_{i,j-1} + \mathbf{g}_y^{t+\Delta t}).\end{aligned} \tag{3.7}$$

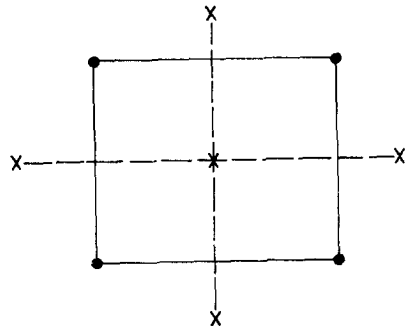

FIG. 1b′

The notation $\mathbf{f}_x^{t+\Delta t}$ expresses the fact that the x-centered difference in $\mathbf{f}$ obtained at time $t + \Delta t$ should be evaluated from the formula:

$$\mathbf{f}_x^{t+\Delta t} = \mathbf{f}(\mathbf{w}_{i+1/2,j+1/2}) - \mathbf{f}(\mathbf{w}_{i-1/2,j+1/2}) + \mathbf{f}(\mathbf{w}_{i+1/2,j-1/2}) - \mathbf{f}(\mathbf{w}_{i-1/2,j-1/2})$$

and similarly for $\mathbf{g}_y^{t+\Delta t}$. Figure 1b′ shows as solid lines the difference approximations to $\mathbf{f}_{,x}$ and $\mathbf{g}_{,y}$ at $t + \Delta t$; the dashed lines are approximations at t. The onedimensional version of this scheme was originally suggested by. Wendroff. This two-step method centers all quantities at the point $(i, j, t + \Delta t/2)$ by the averaging procedure contained in Eq. (3.7), just as is done by the method of Taylor expansion in Eq. (3.1).

For axially symmetric flows, difference equations (3.6) and (3.7) are modified slightly. By inserting the terms

$$\frac{\Delta t}{4}(\mathbf{s}_{k+1/2,l+1/2} + \mathbf{s}_{k+1/2,l-1/2} + \mathbf{s}_{k-1/2,l+1/2} + \mathbf{s}_{k-1/2,l-1/2}) \tag{3.6a}$$

on the right-hand side of Eq. (3.6), and

$$\frac{\Delta t}{2}[\mathbf{s}_{i,j}(t) + \mathbf{s}_{k,l}(t + \Delta t)],\ \mathbf{s}_{k,l}(t + \Delta t) = \tfrac{1}{4}\sum(\mathbf{s}_{i\pm1/2,j\pm1/2})^{t\Delta+t} \tag{3.7a}$$

on the right-hand side of Eq. (3.7), the two-step method can be more ueseful for axially symmetric flows. Equations (3.6a) and (3.7a) center the inhomogeneous term at point $(i, j, t + \frac{1}{2}\Delta t)$ consistent with the other terms in Eqs. (3.6) and (3.7).

Equations (3.6) and (3.7) may be linearized by allowing $\mathbf{f} = \mathbf{Aw}$ and $\mathbf{g} = \mathbf{Bw}$, where $\mathbf{A}$ and $\mathbf{B}$ are considered constant. Then, combining Eqs. (3.6) and (3.7) and substituting $\mathbf{w}(l\Delta x,\ m\Delta y) = \mathbf{w}^0 \exp\,[i(k_x l\Delta x + k_y m\Delta y)]$, one obtains the amplification matrix [5]

$$\begin{aligned}\mathbf{G}' = I &+ i\mathbf{A}\lambda\{\tfrac{3}{4}\sin\xi + \tfrac{1}{4}\sin\xi\cos\eta\} + i\mathbf{B}\lambda\{\tfrac{3}{4}\sin\eta \\ &+ \tfrac{1}{4}\sin\eta\cos\xi\} + \frac{\mathbf{A}^2\lambda^2}{2}(\cos\xi - 1)(1 + \cos\eta) \\ &+ \frac{B^2\lambda^2}{2}(\cos\eta - 1)(1 + \cos\xi) - \frac{\mathbf{AB} + \mathbf{BA}}{2}\lambda^2\sin\xi\sin\eta,\end{aligned} \tag{3.8}$$

where $\xi = k_x\Delta x$, $\eta = k_y\Delta y$ and $\lambda = \Delta t/\Delta x$.

It may be verified that (3.8) can be written as

$$\mathbf{G}' = I + i\lambda\left\{\mathbf{A}\sin\xi\left(\frac{3+\cos\eta}{4}\right) + \mathbf{B}\sin\eta\left(\frac{3+\cos\xi}{4}\right)\right\} - \frac{\lambda^2}{2}\{\mathbf{A}[(1-\cos\xi)(1+\cos\eta)]^{1/2} + B[(1-\cos\eta)(1+\cos\xi]^{1/2}\}^2. \tag{3.9}$$

For $\xi, \eta \ll 1$ the approximations

$$\sin\xi = \xi, \quad 1-\cos\xi = \xi^2/2, \quad 1+\cos\xi = 2-\xi^2/2,$$

may be used. Equation (3.9) becomes

$$\mathbf{G}' = I + i\lambda(\mathbf{A}\xi + \mathbf{B}\eta) - \frac{\lambda^2}{2}(\mathbf{A}\xi + \mathbf{B}\eta)^2 + \mathcal{O}(\xi^3, \eta^3).$$

Then, modulo terms of third order in ξ and η,

$$\mathbf{G}' = \exp[i\lambda(\mathbf{A}\xi + \mathbf{B}\eta)].$$

This is the exact amplification matrix of the differential equation $\mathbf{w}_t = \mathbf{A}\mathbf{w}_x + \mathbf{B}\mathbf{w}_y$. Hence it is clear that the set of Eq. (3.6) and (3.7) are second-order accurate.

4. A Nonlinear Instability

In a recent paper Lax and Wendroff presented a stability proof of the second-order difference method given by Eq. (3.5). We call the amplification matrix associated with the linearized form of Eq. (3.5) $\mathbf{G}$; it is given by

$$\mathbf{G}(\xi, \eta) = I + i(\mathbf{A}\sin\xi + \mathbf{B}\sin\eta) - \mathbf{A}^2(1-\cos\xi) - \mathbf{B}^2(1-\cos\eta) - \left(\frac{\mathbf{AB}+\mathbf{BA}}{2}\right)\sin\xi\sin\eta. \tag{4.1}$$

In order to prove stability one has to show that all eigenvalues of the amplification matrix are ≤ 1 in absolute value (von Neumann condition); this follows if the inner product

$$(\mathbf{Gq}, \mathbf{q}) \leq 1 \tag{4.1'}$$

for all unit vectors $\mathbf{q}$. In fact (4.1') implies that $|\mathbf{G}^n| \leq K$ for integer powers of n, i.e., $n = 1, 2, \ldots$. The difference scheme associated with $\mathbf{G}$ will be stable,

at least if the coefficients of **G** are constant,[3] since the solutions of the difference scheme (obtained by n successive multiplications of the difference operator) will be bounded. This is a consequence of the isometry of the L_2 norm when a Fourier transform is made on the linear difference operator to obtain the amplification matrix. An analysis presented in [2] gives the following inequality:

$$\begin{aligned} |\,(\mathbf{Gq}, \mathbf{q})\,|^2 \leq 1 - |\,\mathbf{Aq}\,|^2(1 - 8\,|\mathbf{Aq}\,|^2)(1 - \cos\xi)^2 \\ - |\,\mathbf{Bq}\,|^2(1 - 8\,|\,\mathbf{Bq}\,|^2)(1 - \cos\eta)^2\,. \end{aligned} \tag{4.2}$$

This expression is less than unity if the requirements

$$\mathbf{A}^2 \leq \tfrac{1}{8}, \qquad \mathbf{B}^2 \leq \tfrac{1}{8},$$

are satisfied. For the case of equal spatial stepsize $\Delta x = \Delta y = \Delta$, this condition can be expressed as

$$\frac{\Delta t}{\Delta} \leq \frac{1}{\sigma^*\sqrt{8}}, \quad \sigma^* = \text{max eigvalue of } \mathbf{A} \text{ or } \mathbf{B}. \tag{4.3}$$

In [1] it was shown empirically that the above stability condition is too stringent; it can be exceeded in practical applications without causing instability; in partic-

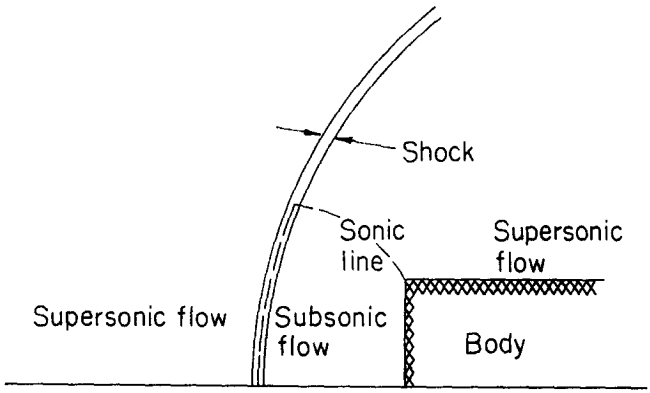

FIG. 1c

[3] Recently, Lax and Nirenberg have shown how to extend this conclusion to **G** with variable coefficients.

ular, $\Delta t/\Delta = 1/\sqrt{2}\sigma^*$, which is twice as large as permitted by (4.3), yielded stable results. It was even possible to go slightly ($\approx 10\%$) beyond this numerical estimate. However, for the class of problems considered in this paper, even satisfying 10% of condition (4.3) led to numerical instability during the early transient portion of the flow (pointwise values of the density ϱ and energy E were $> 10^3$ and $\sim 10^5$, respectively, after which the density became negative). During this time, the shock, having been produced impulsively at the face of the body, was in the process of detaching itself; instabilities were observed in two regions: within the shock close to the axis of symmetry and at the corner of the body. The corner problem could be removed if a first-order difference approximation (discussed in Section 7) was used on the top of the body. But within the shock, negative densities were still obtained.

Figure 2 shows schematically the growth of the solution, at the shock, when an instability is present. The highly oscillatory nature of the solution will grow in time if the calculation is allowed to continue. The data given in Figs. 2 and 3 were

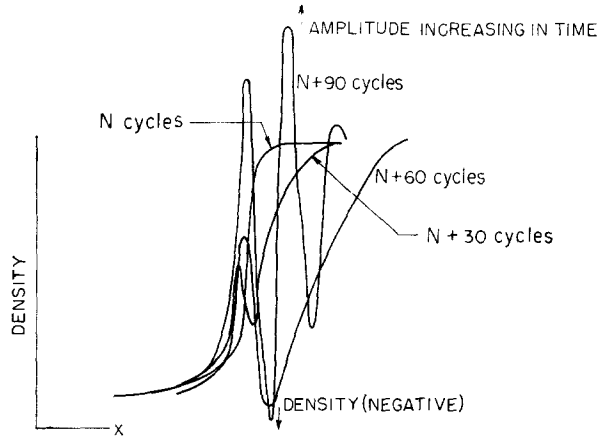

FIG. 2. Schematic of instability occurring within the shock wave for modified Lax–Wendroff scheme; shows growth of $2\Delta x$-component of solution.

obtained from results which were an attempt to eliminate the early instability (after approximately 60 cycles) that was obtained with Eq. (3.5). Here, a modification in the coefficient of the second term [5] in (3.4a), $\lambda/4(\mathbf{A}^+ + \mathbf{A}) \cdot D$, and in (3.4c), $\lambda/4(\mathbf{B}^+ + \mathbf{B}) \cdot D$, where $D > 1$, allowed the calculation to be carried out as far as 500 cycles, but eventually the phenomenon shown in Fig. 2 resulted. For $D > 1$, the accuracy of the difference scheme is no longer second-order.

The result of a case for $D = 3$ is given in Fig. 3, which shows the shock position for successive times. However, at the point where the shock position becomes stationary (at approximately 490 cycles), instability results. Figure 2 shows growth

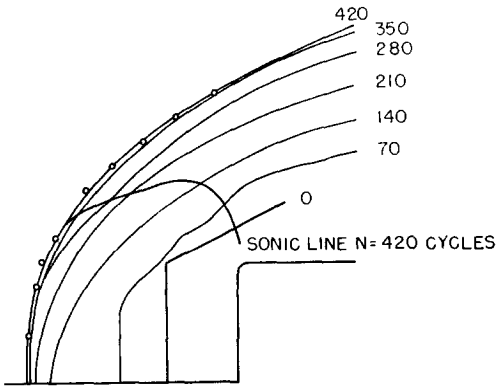

FIG. 3. Time-dependent solution showing shock position for modified Lax–Wendroff scheme. Numbers refer to computational cycles.

of the amplitude of short-wavelength components of the solution for density ϱ. This instability was localized near the axis of symmetry at the shock.

The fourth-order artificial viscosity term which is discussed in [2] was also tested with Eq. (3.5). It had virtually no effect on the stability of the numerical results.

These results were surprising but can be explained by the following argument. Inequality (4.2) together with the stability condition show that the eigenvalues of **G** are, for $\xi, \eta \neq 0$, definitely less than one; this means that high-amplitude waves are damped. However, if $|\mathbf{Aq}|$ and $|\mathbf{Bq}|$ happen to be zero, this damping is absent. Now $|\mathbf{Aq}|, |\mathbf{Bq}|$ can vanish if and only if zero is an eigenvalue of **A** of **B**. The eigenvalues of **A**, **B** are $u \pm c$, u and $v \pm c$, v. Hence, for points, lines, or surfaces in the flow where

$$\text{Condition I:} \quad u/c = 1 \text{ and } \eta = 0, \text{ or } v/c = 1 \text{ and } \zeta = 0$$

(c is the local sound speed), or

$$\text{Condition II:} \quad u = 0 = v,$$

one of the eigenvalues becomes zero. Condition I corresponds to local one-di-

mensional sonic flow, and Condition II corresponds to flow at stagnation points. If the sonic line is extended, it will pass within the shock (see Fig. 1c) so that near the axis of symmetry, since the flow is locally one-dimensional, $\eta = 0$, Condition I occurs; i.e., there will be no damping for the associated linear difference scheme (4.2), and hence $|(\mathbf{Gq}, \mathbf{q})|^2 = 1$. Since this condition of neutral stability occurs in a part of the flow where the basis of applying linear analyses is weakest (where flow properties vary most rapidly), a statement of nonlinear stability is suspect. Such second-order schemes [including the two-step method given by Eqs. (3.6) and (3.7)] will probably need additional damping terms for successful results. These terms must be third-order so as to preserve the numerical accuracy.

Based upon this explanation, it becomes clear that the oscillations experienced in the previous calculation [1] of Mach reflection resulted from a nonlinear instability. In the case of oblique reflection there are no sonic lines and there were no oscillations observed. As the calculation proceeded, the properties at all data points converged to 6 places. The higher the free stream Mach number, the faster the convergence. However, for Mach reflection, a "sonic line" (Condition I) coincides with the normal shock and the slip line. Here the calculation converged slowly and oscillations were present in the region between the shock and the downstream boundary. For very low Mach-number values, $M \leq 1.4$, the solution never converged.

The next section shows that a third-order viscosity in two dimensions can be introduced.

5. Artificial Viscosity in Two Dimensions

We have seen that, in regions of flow which are locally one-dimensional, instability can result at the shock wave which separates the supersonic region from the subsonic region or in the region of stagnation point flow. In order to damp oscillations which might be generated at the shock, an artificial viscosity, which is quadratic, will be added to the basic difference scheme. This will ensure that only at points where rapid variations occur will the viscosity influence the solution. When the solution tends to constancy the viscosity should vanish. These conditions allow the viscosity to be expressed in terms of two neighboring net points which are at states ω and ω', i.e., viscous term $\sim \mathbf{Q}(|\omega - \omega'|) \cdot (\mathbf{w}(\omega) - \mathbf{w}(\omega'))$. We choose to write the viscosity in terms of the two additive factors

$$\frac{\Delta t}{2} \Delta_x(\mathbf{Q}^x(\omega, \omega')\Delta_x'\mathbf{w}) + \frac{\Delta t}{2} \Delta_y(\mathbf{Q}^y(\omega, \omega')\Delta_y'\mathbf{w}) . \tag{5.1}$$

The undivided forward difference in the x- and y-direction is represented by the

operators Δ_x' and Δ_y'. It is reasonable to express $\mathbf{Q}^x(\omega, \omega')$ and $\mathbf{Q}^y(\omega, \omega')$ in terms of the matrices $\mathbf{A}$ and $\mathbf{B}$ so that (5.1) will be dimensionally correct, hence

$$\mathbf{Q}^x = \sum a_n \mathbf{A}^n, \qquad \mathbf{Q}^y = \sum b_n \mathbf{B}^n, \qquad n = 0, 1, 2. \tag{5.2}$$

We have not included cross terms in the viscosity since it is expected that their behavior will not contribute substantially within the shock, especially if the shock is locally one-dimensional.

We choose the coefficients a_i, b_i, $i = 0, 1, 2$, as follows: Let $\sigma_i(\mathbf{A})$, $i = 1, 2, 3$, represent the eigenvalues of $\mathbf{A}(u \pm c, u)$; and $\sigma_i(\mathbf{B})$, $i = 1, 2, 3$, the eigenvalues of $\mathbf{B}(v \pm c, v)$. Then coefficients α_i are written as differences of the eigenvalues $\sigma(\mathbf{A})$:

$$\alpha_i = \frac{1}{2} \varkappa_i \frac{|\sigma_i(\omega) - \sigma_i(\omega')|}{(\bar{\sigma}_i - \bar{\sigma}_j)(\bar{\sigma}_i - \bar{\sigma}_k)}, \quad i = 1, 2, 3, \quad j \neq i, \quad k \neq i, j. \tag{5.3a}$$

Here the barred quantities are understood to be averages over the enterval (ω, ω'), and $\varkappa_i$ may be a function of σ or constant. This will ensure that if the flow is locally constant the α_i will vanish. A similar relationship can be written for β_i in terms of $\sigma(\mathbf{B})$. With this choice for α and β, the coefficients of Eq. (5.2) can be put in the form

$$\begin{aligned} a_0 &= \sum_{i=1, j\neq i, k\neq i, j}^{3} \alpha_i \sigma_j \sigma_k, \\ a_1 &= -\sum_{i=1, j\neq i, k\neq i, j}^{3} \alpha_i (\sigma_j + \sigma_k), \\ a_2 = 0 &= \sum_{i=1}^{3} \alpha_i. \end{aligned} \tag{5.3b}$$

Then the matrices defined in (5.2) can be given by

$$\begin{aligned} \mathbf{Q}^x &= \sum_{i=1, j\neq i, k\neq i, j}^{2} \alpha_i \{(\bar{\mathbf{A}} - \bar{\sigma}_j I)(\bar{\mathbf{A}} - \bar{\sigma}_k I), \\ \mathbf{Q}^y &= \sum_{i=1, j\neq i, k\neq i, j}^{2} \beta_i (\bar{\mathbf{B}} - \bar{\sigma}_j I)(\bar{\mathbf{B}} - \bar{\sigma}_k I)\}. \end{aligned} \tag{5.4}$$

It is clear that, with such a choice of coefficients the eigenvalues or $\mathbf{Q}^x$ of $\mathbf{Q}^y$ will be proportional to the difference of the eigenvalues of $\mathbf{A}$ or $\mathbf{B}$ in the interval (ω, ω'), i.e.,

$$\mathbf{Q} = \tfrac{1}{2} \varkappa_i |\sigma_i(\omega) - \sigma_i(\omega')| \cdot I.$$

Hence, since there will always be at least one nonzero eigenvalue, the viscosity will contribute to the solution in regions where the solution varies most rapidly. This will ensure us that the difference scheme will have dissipation.

Therefore the complete difference scheme obtained by combining Eq. (3.5) with the artificial viscosity given by Eq. (5.1) is

$$\begin{aligned}\mathbf{w}(t+\Delta t) = \mathbf{w}(t) + \lambda\{&D_x[L_x\mathbf{C}(x) + \tfrac{1}{2}\,\mathbf{Q}^x D_x'\mathbf{w}] \\ &+ D_y[L_y\mathbf{C}(y) + \tfrac{1}{2}\,\mathbf{Q}^y D_y'\mathbf{w}]\}.\end{aligned} \tag{5.5}$$

We have used $L_x\mathbf{C}(x) = \frac{1}{2}\{\mathbf{C}(x+\Delta x) + \mathbf{C}(x)] = \mathbf{C}(\Delta x/2)$ as the forward averaging operator, and D_x and D_x' as the centered and forward difference operators, respectively.

For the Lagrangian system of hydrodynamic equations these coefficients reduce to that given by Lax and Wendroff, i.e.,

$$a_0 = 0 = a_1\,,$$

$$a_2 = \frac{1}{2}\,\varkappa\,\frac{|\,c(\omega) - c(\omega')\,|}{\bar{c}^2}\,.$$

In the next section we use this Lagrangian form of the viscosity to show stability of the Lax–Wendroff scheme with the added artificial viscosity.

6. Stability Analysis of Second-Order Scheme with Viscosity

In order to study the stability of the difference schemes we first linearize the equations by taking the matrices **A** and **B** to be locally constant. We assume that the real matrices **A**, **B** are symmetric or at least they can be symmetrized by a similarity transformation. Also, for simplicity, let $\Delta x = \Delta y = \Delta t = 1$. We also take the viscosity to be of the form

$$\mathbf{Q}(\mathbf{A},\mathbf{B}) = \mathbf{Q}^x(\mathbf{A}) + \mathbf{Q}^y(\mathbf{B}) = \tfrac{1}{2}\,\alpha\,\mathbf{A}^2 + \tfrac{1}{2}\,\beta\,\mathbf{B}^2\,, \tag{6.1}$$

where α and β are constant. This choice of **Q** is then substituted into (5.1) and the result is linearized, i.e., $\frac{1}{2}\,\alpha\,\mathbf{A}^2\,D_x^2\,\mathbf{w} + \frac{1}{2}\,\beta\,\mathbf{B}^2\,D_y^2\,\mathbf{w}$, where the second difference operator is represented by D^2. Take the Fourier transform of the above and add it to the amplification matrix given by Eq. (4.1); the result is

$$\begin{aligned}\mathbf{G}(\xi,\eta) = I + i(\mathbf{A}\sin\xi + \mathbf{B}\sin\eta) - (1 + \tfrac{1}{2}\,\alpha)\mathbf{A}^2(1-\cos\xi) \\ - \left(1 + \frac{1}{2}\,\beta\right)\mathbf{B}^2(1-\cos\eta) - \frac{\mathbf{AB}+\mathbf{BA}}{2}\sin\xi\sin\eta\,.\end{aligned} \tag{6.2}$$

The proof basically parallels that presented by Lax and Wendroff [2]; we give all steps for completeness.

We wish to estimate the quantity $(\mathbf{Gq}, \mathbf{q})$ for all unit vectors $\mathbf{q}$. $\mathbf{G}$ is separated into its real and imaginary parts

$$\mathbf{G} = \mathbf{X} + i\mathbf{Y},$$

where

$$\mathbf{Y} = \mathbf{A} \sin \xi + \mathbf{B} \sin \eta$$

and

$$\mathbf{X} = \mathbf{I} - \mathbf{R}$$

with

$$\mathbf{R} = \left(1 + \frac{1}{2}\alpha\right)\mathbf{A}^2\Theta + \left(1 + \frac{1}{2}\beta\right)\mathbf{B}^2\Phi + \frac{\mathbf{AB} + \mathbf{BA}}{2} \sin \xi \sin \eta. \tag{6.3}$$

We have used the definitions $\Theta = 1 - \cos \xi$ and $\Phi = 1 - \cos \eta$. Now

$$(\mathbf{Gq}, \mathbf{q}) = (\mathbf{Xq}, \mathbf{q}) + i(\mathbf{Yq}, \mathbf{q}).$$

Since $\mathbf{A}$ and $\mathbf{B}$ are real and symmetric, it follows that $\mathbf{X}$ and $\mathbf{Y}$ are real and symmetric; hence

$$|(\mathbf{Gq}, \mathbf{q})|^2 = (\mathbf{Xq}, \mathbf{q})^2 + (\mathbf{Yq}, \mathbf{q})^2. \tag{6.4}$$

$\mathbf{R}$ can be given by the identity

$$\mathbf{R} \equiv \tfrac{1}{2}\mathbf{A}^2\Theta^2 + \tfrac{1}{2}\mathbf{B}^2\Phi^2 + \tfrac{1}{2}\mathbf{Y}^2 + \tfrac{1}{2}\alpha\mathbf{A}^2\Theta + \tfrac{1}{2}\beta\mathbf{B}^2\Phi. \tag{6.5}$$

The proof proceeds by computing the right-hand side of Eq. (6.4). By using the abbreviations $x = (\mathbf{Xq}, \mathbf{q})$, $y = (\mathbf{Yq}, \mathbf{q})$, and $r = (\mathbf{Rq}, \mathbf{q})$, the absolute value of the real part of the inner product of the amplification matrix is

$$x^2 = (1 - r)^2 = 1 - 2r - r^2. \tag{6.6}$$

Now the identity in $\mathbf{R}$, Eq. (6.5), is used to obtain the second term in Eq. (6.6), and the definition of $\mathbf{R}$, given by Eq. (6.3), is used for the evaluation of r^2. Taking the inner product of Eq. (6.5) and using the Schwartz inequality $(Y^2\mathbf{q}, \mathbf{q}) = |Y\mathbf{q}|^2 \geq y^2$, we obtain

$$r \leq \tfrac{1}{2}\mathbf{A}^2\Theta^2 + \tfrac{1}{2}\mathbf{B}^2\Phi^2 + \tfrac{1}{2}y^2 + \tfrac{1}{2}\alpha\mathbf{A}^2\Theta + \tfrac{1}{2}\beta\mathbf{B}^2\Phi. \tag{6.7}$$

To obtain $|(\mathbf{Rq}, \mathbf{q})|^2$, multiply Eq. (6.3) by $\mathbf{q}$ and form the inner product. One

of the resulting terms, $\mathrm{Re}(\mathbf{Aq}, \mathbf{Bq}) \sin\xi \sin\eta$, may be estimated by the Schwartz inequality

$$\leq |\,\mathbf{Aq}\,|\;|\sin\xi|\;|\,\mathbf{Bq}\,|\;|\sin\eta| \leq 2\,\{|\,\mathbf{Aq}\,|^2\,\Theta + |\,\mathbf{Bq}\,|^2\Phi\}\,.$$

The trigonometric inequalities $\Theta \geq \frac{1}{2}\sin^2\xi$ and $\Phi \geq \frac{1}{2}\sin^2\varphi$ have been used. Using this result, we conclude that

$$r \leq |\,\mathbf{Aq}\,|^2\,(2 + \tfrac{1}{2}\alpha)\,\Theta + |\,\mathbf{Bq}\,|^2\,(2 + \tfrac{1}{2}\beta)\,\Phi$$

or

$$\begin{aligned} r^2 \leq (|\,\mathbf{Aq}\,|^2)^2\,\Theta^2 &\left\{\left(2 + \frac{\alpha}{2}\right)^2 + \left(2 + \frac{\alpha}{2}\right)\left(2 + \frac{\beta}{2}\right)\right\} \\ &+ (|\,\mathbf{Bq}\,|^2)^2\,\Phi\left\{\left(2 + \frac{\beta}{2}\right)^2 + \left(2 + \frac{\beta}{2}\right)\left(2 + \frac{\alpha}{2}\right)\right\}. \end{aligned} \tag{6.8}$$

Substituting Eqs. (6.8) and (6.7) into Eq. (6.6) gives

$$\begin{aligned} x^2 + y^2 \leq 1 &- |\,\mathbf{Aq}\,|^2\,\{(1 + \alpha) - \alpha^1\,|\,\mathbf{Aq}\,|^2\}\,\Theta^2 \\ &- |\,\mathbf{Bq}\,|^2\,\{(1 + \beta) = -\beta^1\,|\,\mathbf{Bq}\,|^2\}\,\Phi^2\,. \end{aligned} \tag{6.9}$$

We have used the trigonometric inequalities (for $\xi, \eta \sim \pi$) $\Theta^2 \geq \Theta$ and $\Phi^2 \geq \Phi$ (short-wavelength disturbances must be damped so that their growth will not affect the numerical solution; see Fig. 2) to obtain Eq. (6.9). The right-hand side is less than one if

$$|\,\mathbf{Aq}\,|^2 = |\,\sigma(\mathbf{A})\mathbf{q}\,|^2 \leq \frac{1 + \alpha}{\alpha^1}\;;\quad |\,\mathbf{Bq}\,|^2 = |\,\sigma(\mathbf{B})\mathbf{q}\,|^2 \leq \frac{1 + \beta}{\beta^1}\,. \tag{6.10}$$

α^1 and β^1 are abbreviations for the quantities in brackets in Eq. (6.8).

It is interesting to note that Eq. (6.9) is of the same form as Eq. (4.2). The argument presented in Section 4 on nonlinear stability would appear to hold in the present case. It must be concluded [in light of the numerical experiments performed with Eq. (5.5)] that linearization eliminates many important features of the difference scheme, e.g., nonlinear terms (see Richtmyer and Morton [7]). For the simple case of equal coefficients for the viscosity, Eq. (6.10) becomes

$$\sigma^2(\mathbf{A}) \leq \frac{1 + \alpha}{2(2 + \alpha/2)^2} = f(\alpha)\,.$$

The max of $f(\alpha)$ is for $\alpha = 2$, $f(2) = \frac{1}{8}$. Hence there is hope that the scheme will be stable for

$$\frac{\Delta t}{\Delta x} | \sigma(\mathbf{A}) | \leq \frac{1}{\sqrt{6}}, \tag{6.11}$$

while a similar expression holds for $\sigma(\mathbf{B})$.[4] This is somewhat larger than the value $1/\sqrt{8}(\alpha = 0)$ obtained by Lax and Wendroff. The term given by Eqs. (5.1) and (6.1), which is an artificial viscosity, clearly has a stabilizing influence on the difference scheme Eq. (3.5), since the allowable time increment is larger. Similar results hold for the more complicated forms of viscosity used in the numerical calculation, i.e., Eqs. (5.1) and (5.2).

The test of the stability condition was made using a constant to represent the right-hand side of (6.11). This numerical value was fed into the IBM 7094 via a data card and the resulting solution was checked every 30 cycles of computation. No other changes were made and the results appear in Table I. The theoretical limit $r < .408$ (which is close to the Lax Wendroff value of .354) agrees within the accuracy obtained with the numerical estimate of Table I. Additional experiments will be performed, especially for the case of axially symmetric flows.

TABLE I

$r = \| \sigma \|_{\max} \Delta t/\Delta$	Condition
.65	Unstable at 90 cycles (negative densities)
.55	Negative velocities at 350 cycles near stagnation point
.45	Negative velocities at 640 cycles near stagnation point
.35	No negative densities or velocities at 2500 cycles

The fact that the velocities became negative for some values of r is in itself not an instability. The solution in the region of the stagnation point did start to diverge from the known solution when negative velocities were observed. As the compu-

[4] Although α and β are not arbitrary constants but depend on the solution about which linearization is performed, locally the stability limit imposed by Eq. (4.3) may be relaxed for the condition given by Eq. (6.11). In practical applications, however, the difference is unimportant and Eq. (4.3) may be used.

tation proceeded the situation became worse since the negative values of the x-component of velocity propagated into the mesh from the stagnation point. At this point the calculation for the case was terminated.

7. Numerical Results

The results of two calculations are presented. The difference scheme (5.5), which includes the artificial viscosity (5.1), was used to obtain these results. The coefficient $\varkappa$ in Eq. (5.3a) was initially set equal to 2, but during the course of the calculation it was reduced to 1; also $\Delta x = \Delta y = \Delta = 1$. The free-stream Mach number is 4.3, and γ, the ratio of specific heats, is 1.4. The flow was started impulsively by using the free-stream conditions as initial data. In Fig. 4 we plot

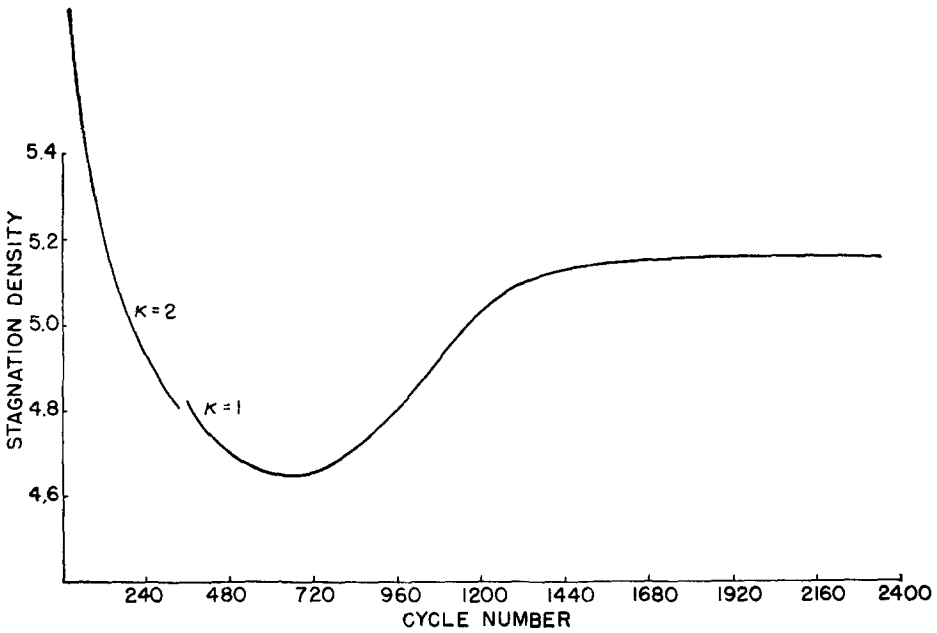

FIG. 4. Convergence of time-dependent solution. Stagnation density ($M = 4.3$, $\gamma = 1.4$).

stagnation density vs. number of cycles. Beyond the 2340th cycle the values of density everywhere in the flow field are constant to four figures; clearly the method converges. However, the shock standoff position assumed a steady value after approximately several hundred cycles of computation. The accuracy

in the calculation of the stagnation density is exceptionally good while the error of 0.96% in the computed stagnation pressure is consistent for the method. Figure 5 shows the density for values of y as a function of x. The

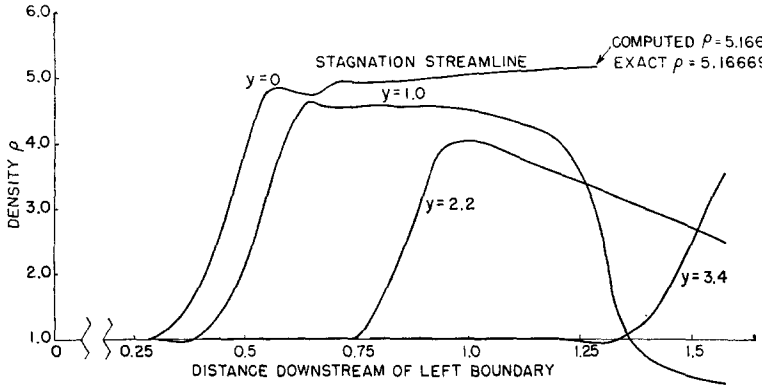

FIG. 5. Density distribution along some coordinates y = constant, normalized with body radius, $M = 4.3$, $\gamma = 1.4$.

abscissa in Figs. 5 and 10 have been normalized so that 1 occurs at mesh point 14. The distance y has been normalized by the radius of the body. The corner of the body is at $x = 1.28$. For $y = 1$, it is seen that there is a rapid variation of the density corresponding to the corner expansion. For $y = 2.2$, the density, after the shock, decreases linearly, corresponding to the fluid expanding past the body. The complete flow field is shown in Fig. 6; the values on the abscissa correspond to the positions of the mesh points. Here the position of the shock and sonic line are shown with respect to the body. The dashed curve represents the sonic line computed with the scheme of Lax given in 1952.

$$\mathbf{w}(t + \Delta t) = \mathbf{w}(t) + \lambda(D_x\mathbf{f} + D_y\mathbf{g}) + \Delta^2(D_x^2\mathbf{w} + D_y^2\mathbf{w}). \tag{7.1}$$

Equation (7.1) is a first-order method. When using this difference scheme, the point of attachment of the sonic line to the body is greater than 3 space increments from the body corner. This difference method has an effective artificial viscosity coefficient which varies as Δt^{-1}. Hence its use is only practical for large time steps, and, even using the largest allowable stepsize, the smearing effect is substantial, i.e., the shock width may be $\sim 15\Delta x$. On the other hand the high-order scheme, Eq. (5.5), gives the position of the sonic line correctly, i.e., within a fraction of one mesh point of the corner, while the shock width is given over two or three cells.

As shown in Fig. 7, the Mach number at the corner is 0.975. One mesh point to the right on top of the body the Mach number is 2.04, but it is 0.666 one mesh point below the corner, on the body face (in these calculations the body face was defined by 10 increments). Beyond the corner the Mach number increases very rapidly, indicating a strong rarefaction wave.

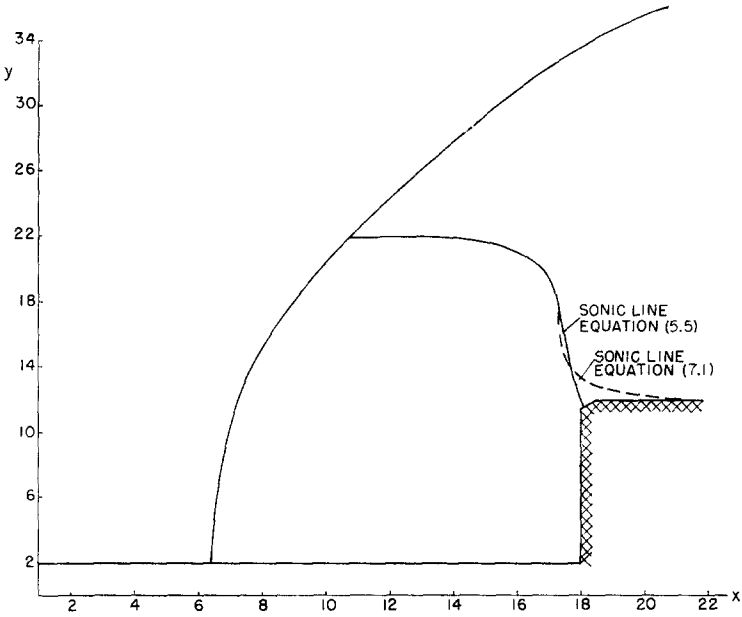

FIG. 6. Flow field showing detached shock and sonic line for $M = 4.3$, $\gamma = 1.4$; detachment distance = 1.16.

Thus the difference scheme is able to handle such rapid variations of the flow quantities; this is again indicated by the distribution of pressure ratio along the body given in Fig. 8. In Fig. 9 the entropy distribution along the stagnation streamline is shown. The theoretical value of entropy at the stagnation point can be calculated exactly; it is 2.24, and the computed value is 2.20. The abrupt entropy change near the corner and the oscillation on top of the body are very likely due to the fact that the vertical component of velocity was computed on the top of the body rather than prescribed to be zero. This was done so as to observe the number of space steps needed to approach the correct value. This meant that improper values of entropy, mass, etc., were introduced into the flow because of false boundary conditions. The entropy distribution Δ above the body is shown and it approaches the theoretical correct value. The sharp rise in the value of the

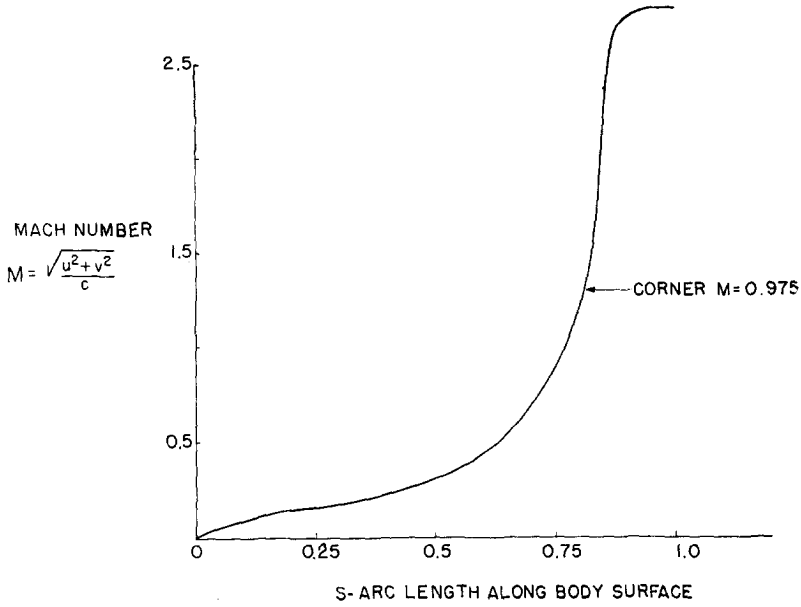

FIG. 7. Mach number distribution along blunt body, $M = 4.3$, $\gamma = 1.4$.

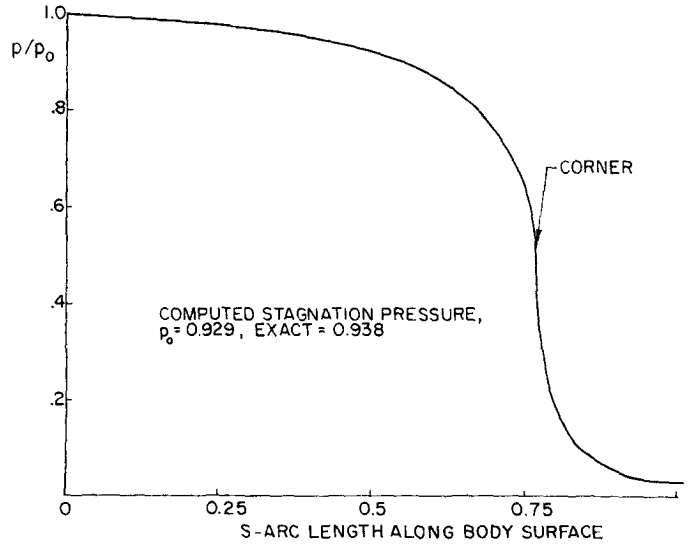

Fig. 8. Pressure ratio along blunt body. $M = 4.3$, $\gamma = 1.4$.

entropy at the corner is presumably due to the artificial viscosity acting on the steep rarefaction gradients at the corner. The artificial viscosity could not be switched off in this region, especially at the corner. Since the rarefaction wave

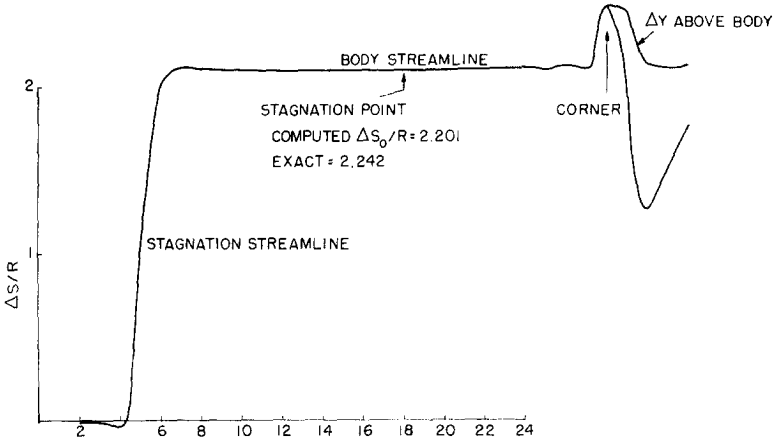

FIG. 9. Entropy distribution along stagnation streamline and body streamline.

is centered at this point on the body, the numerical solution behaves like a "rarefaction shock" (a sharp decrease in density and pressure) with an attendant undershoot eventually leading to negative densities. In order to resolve this problem, additional work is necessary. Figures 10 and 11 show some results for the case in which $M = 10$ and $\gamma = 1.17$. In this calculation it was found necessary to introduce the function

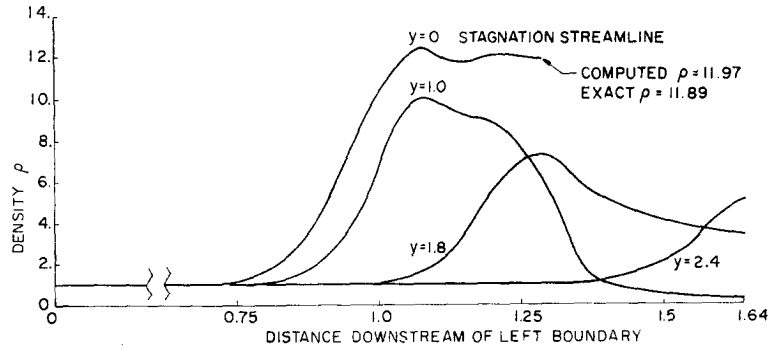

FIG. 10. Density distribution along some coordinates y = constant, normalized with body radius $M = 10$, $\gamma = 1.17$.

$$\varkappa = \varkappa_0 \{1 + \exp(1 - |\mathbf{u}| / \varkappa_1)\} \quad \text{if} \quad |\mathbf{u}| / \varkappa_1 \leq 1,$$

or

$$\varkappa = 1 \qquad \text{otherwise;}$$

for the coefficient of viscosity given in Eqs. (5.3a), $\varkappa_1$ was chosen to be of the order of the velocity behind the strong normal shock, while $\varkappa_0$ was between one half and one; $|\mathbf{u}|$ is the magnitude of the velocity. Using this form for the viscosity coefficient has the effect of providing additional damping near the stagnation point. This damping was not required for the previous case ($M = 4.3$) since the

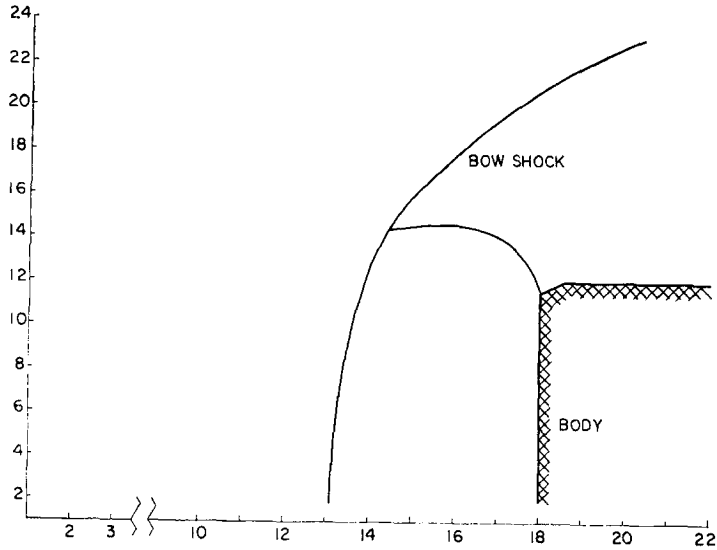

FIG. 11. Flow field showing detached shock and sonic line for $M = 10$, $\gamma = 1.17$; detachment distance = 0.49.

shock was well away from the body. It is felt, for the case $M = 10$, that if unequal spacing were chosen in the x-direction, so that there would be more steps between the shock and the body, additional damping would be unnecessary.

AKNOWLEDGMENTS

The author would like to acknowledge that during the course of this investigation he had many helpful discussions with Professor Peter Lax — all of which made this work possible. I also thank Professor Robert Richtmyer for his comments on the paper.

References

1. Samuel Z. Burstein, *AIAA J.* **2**, 211–217 (1964).
2. Peter D. Lax and Burton Wendroff, *Commun. Pure Appl. Math.* **17**, 381–398 (1964).
3. Peter D. Lax and Burton Wendroff, *Commun. Pare Appl. Math.* **13**, 217–237 (1960).
4. Robert Richtmyer, "A Survey of Difference Methods for Non-Steady Gas Dynamics." *NCAR Tech. Note* **63-2**.
5. Robert Richtmyer, "Difference Methods for Initial-Value Problems." Wiley (Interscience), New York (1957).
6. H. U. Thommen and L. D'Attore, "Calculation of Three Dimensional Supersonic Flow Fields by a Finite Difference Method," General Dynamics/Astronautics, GDA-ERR-AN539, September 1964.
7. R. D. Richtmyer and K. W. Morton, "Stability Studies for Difference Equations," NYO 1840–5, August 25, 1964.